Radius of Gyration of Polystyrene Combs and Centipedes in Solution

Yo Nakamura,*,†,§ Yunan Wan,† Jimmy W. Mays,*,† Hermis Iatrou,‡ and Nikos Hadjichristidis‡

Department of Chemistry, University of Alabama at Birmingham, Birmingham, Alabama 35294; and University of Athens, Panepistimiopolis, 15771 Athens, Greece

Received April 21, 2000; Revised Manuscript Received August 8, 2000

ABSTRACT: The method of Iatrou et al. (*Macromolecules* **1998**, *31*, 6697) was applied to synthesize a normal comb polystyrene sample with uniform side chains equally spaced along the main chain but with the most probable distribution in the main chain length. The molecular weights of the side chain and the connector (the part of the main chain between the neighboring side chains) were 3.5×10^4 and 2.3×10^4, respectively. The sample was analyzed using a gel-permeation chromatography system with a multiangle light scattering and refractive index detector to determine the relationship between the *z*-average mean square radius of gyration $\langle S^2 \rangle$ and the weight-average molecular weight M_w. Tetrahydrofuran (THF) was chosen as the solvent. The relation fell considerably below that for linear polystyrene. The slope of the plot of $\log \langle S^2 \rangle^{1/2}$ vs $\log M_w$ for the comb polymer was 0.46, a value much smaller than the Flory exponent 0.6 for linear chains in good solvents. Similar measurements were also made on polystyrene centipedes prepared by Iatrou et al., which have two side chains at each junction point. As the ratio r of the molecular weight of the side chain to that of the connector increased, the $\langle S^2 \rangle$ vs M_w relation was lowered. Comparison of the experimental relationship with theoretical predictions for flexible discrete chains suggested that the main chains of the two types of polymer are stiffened by the crowding of the side chains. To estimate the backbone stiffness, $\langle S^2 \rangle$ was calculated on the basis of the wormlike comb model whose main and side chains have different Kuhn lengths λ^{-1} and λ_s^{-1}, respectively. With $\lambda_s^{-1} = 2$ nm and the linear mass density $= 390$ nm^{-1} (for both main chain and side chains), λ^{-1} was estimated so as to give the closest agreement between the calculated and measured $\langle S^2 \rangle$. It was found that the calculated values for the comb polymer with $\lambda^{-1} = 5.5$ nm agree closely with the experimental data. The data for the centipedes were also explained by the theory, which showed the backbone stiffness to increase with increasing r.

Introduction

An important finding in recent polymer solution studies is that polymacromonomers which have comb structures behave as stiff chains in solution,[1−7] despite being composed of such flexible components as polystyrene. Their stiffness increases when the side chain becomes longer and/or when the solvent becomes thermodynamically better.[2,4−6] The stiffness may be considered to arise from repulsions between neighboring side chains.[8] If this hypothesis is accepted, the stiffness should be reduced with decreasing the distance (spacer length) between neighboring side chains. In polymacromonomers, however, the spacer length is fixed by two C−C bonds, and thus we have to use some different synthetic strategy to obtain comb polymers with different spacer lengths.

Some groups[9−13] previously prepared comb polymers by grafting reactions of anionic living polymer chains onto active sites along the main chain and found from light scattering that measured *z*-average mean square radii of gyration $\langle S^2 \rangle$ were larger than those expected from theories based on the Gaussian bond probability. They considered the comb polymers to be expanded due to the high segment densities. However, no attempt was made to estimate the stiffness of the polymers in such early days. For an unequivocal determination of the chain stiffness of a given comb polymer, we need a series of samples with different main chain lengths and a fixed side chain length. The grafting reaction is not always advantageous to this end, in that it is not completed since high side chain densities prevent additional side chains from approaching the active groups on the main chain.[14]

Very recently, Iatrou et al.[15] made comblike polymers using a new scheme, in which two side chains connected by tetrachlorosilane were reacted with α,ω-dianionic polymer chains (connectors) in a polycondensation manner. This method allows us to obtain comb polymers with fixed side chain lengths but broad (most probable) distribution in the main chain length, i.e., a series of samples with different molecular weights after fractionation. The comblike polymers prepared by Iatrou et al. have two side chains connected at each junction point and are called "centipedes" ("a" in Figure 1).

In this work, we synthesized a normal comb polystyrene sample with one side chain at each junction point ("b" in Figure 1) following the method of Iatrou et al., and determined $\langle S^2 \rangle$ of the polystyrene comb and the centipedes made by Iatrou et al., all in tetrahydrofuran (THF) as functions of weight-average molecular weight M_w using a multiangle laser-light-scattering (MALLS) detector equipped with a gel-permeation chromatography (GPC) separation system. This technique is especially powerful for obtaining such data from a polymer sample with very wide molecular weight distribution. The $\langle S^2 \rangle$ data obtained are analyzed by use of relevant expressions derived to examine the effect of the degree of branching on chain stiffness.

* To whom correspondence should be addressed.
† University of Alabama at Birmingham.
‡ University of Athens.
§ Permanent Address: Department of Macromolecular Science, Osaka University, Machikaneyama-cho 1−1, Osaka 560-0043, Japan.

10.1021/ma0007076 CCC: $19.00
Published on Web 10/04/2000

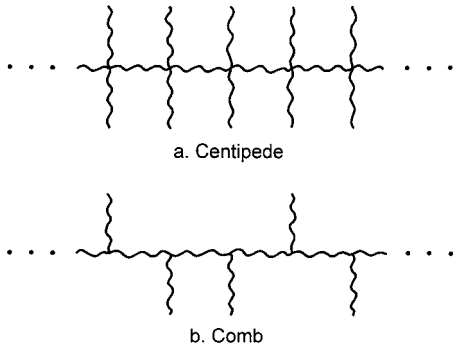

Figure 1. Schematic representation of centipede and comb molecules.

Experimental Section

Polymer Samples. We used three centipede polystyrene samples previously prepared by Iatrou et al.[15] In addition, one sample of normal comb polystyrene was synthesized as follows. Linear polystyrene for the side chains was synthesized in benzene using *sec*-butyllithium as the initiator and reacted with excess trichloromethylsilane after adding about 2 units of butadiene at each end. The polystyrene connector was made using (1,3-phenylene)bis(3-methyl-1-phenylpentylidene)dilithium as the difunctional initiator in benzene with a small amount of THF added to avoid the aggregation of the initiator and growing chain ends. This initiator was obtained by the reaction of 1,3-bis(1-phenylethenyl)benzene with *sec*-butyllithium. After the solvent was replaced with pure benzene (to reduce the 1,2 addition), about 2 units of butadiene were introduced at each end to promote the efficiency of the polycondensation reaction (when we once skipped this step, we obtained only linear chains made of a connector and two arms, because the steric hindrance among benzene rings at the chain ends prevented the linkage of more than two chains at the junction point). The solution of the side chains was poured dropwise into the connector solution after adding a small amount of THF; to make the samples' molecular weight as high as possible, almost equal amount of the side chains and the connector were mixed. The reaction was monitored by GPC with an aliquot of the solution taken into an ampule.

The GPC chromatograms "A" and "B" in Figure 2 show the peaks for the side chain and the connector, respectively. Here, V_e denotes the elution volume. A small subpeak in "A" shows that some dimers are contained but these species do not affect the polycondensation reaction. A similar subpeak, which can also be seen in "B", indicates the presence of the subproduct produced by the deactivation of one living site of the difunctional initiator due to some impurity. This product may terminate the polycondensation reaction. However, since its amount is very small, the effect was not serious.

The GPC chromatogram "C" shows the peak for the product after mixing "A" and "B". A broad peak for the polycondensation product can be seen at $V_e \approx 22$ cm^3. The shoulder at $V_e \approx 23.5$ shows the linear product made of a connector joining two arms. After a couple of days, we added some more side chains to ensure the completion of the reaction, and obtained the final product "D". This comb polystyrene sample was designated as CS25−35.

The weight-average molecular weights of the side chain and the connector (M_{side} and M_{con}, respectively) determined by light scattering measurements are shown in Table 1, along with the ratio r ($=M_{side}/M_{con}$). The values for the centipede polystyrene samples[15] are also included in the table.

Light-Scattering Measurements. Light-scattering measurements were made at room temperature using a MALLS detector DAWN DSP-6 (Wyatt Technology Inc.) with He−Ne laser (633 nm). The photometer, which was calibrated with pure toluene, was connected to a GPC system equipped with three columns (two Waters HT6E linear columns and 1 Waters HT3 column (10^3Å)) and a refractive index (RI) detector (Waters 2410) which was used to determine the concentration at each position of the peak. THF was used as the eluent; the flow rate was set to 1 mL/min. Polymer sample solutions with mass concentrations of about 1×10^{-3} g cm^{-3} were injected using a sample loop of 0.1 cm^3 capacity.

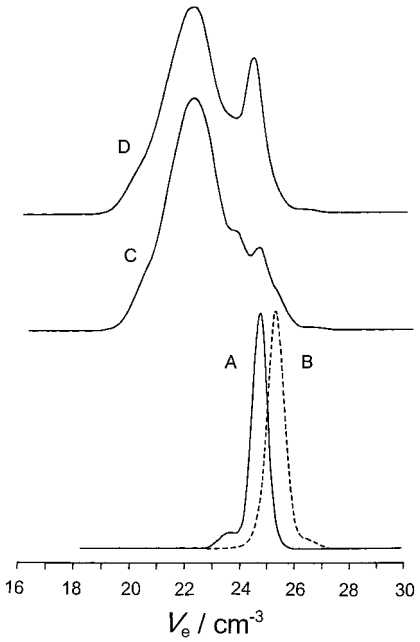

Figure 2. GPC chromatograms for the side chain (A), connector (B), middle product (C), and the final product (D) of comb polystyrene CS25−35.

Table 1. Molecular Parameters for Polystyrene Comb and Centipedes

	M_{side}	M_{con}	r
CS25−35	35100	23100	1.52
GS15−35[a]	34400	15700	2.19
GS40−25[a]	28800	41200	0.70
GS60−15[a]	13500	57000	0.24

[a] Reference 15.

Table 2. Values of the Radius of Gyration for Linear Polystyrene in THF

$M_w \times 10^{-5}$	$\langle S^2 \rangle^{1/2}$/nm
17.2	66.1
8.18	40.8
7.01	37.7
5.16	31.2
3.51	25.1

The angular dependence of the scattering intensity was analyzed using Berry's square-root plot to determine $\langle S^2 \rangle$ at each position of the peak. The specific refractive index increment for THF solutions was taken to be 0.186 cm^3 g^{-1}.[16]

Measurements were also made on Pressure Chemical's standard polystyrene samples. The values of $\langle S^2 \rangle$ and M_w for five samples were determined by the integration of the RI signal and scattering intensity at each scattering angle over the whole peak area. The results are presented in Table 2.

Results

Figure 3 depicts the curves of the polymer mass concentration c, M_w, and $\langle S^2 \rangle$ against V_e for CS25−35. It can be seen that the concentration is diluted down to $c \approx 2 \times 10^{-4}$ g cm^{-3} after passing through the columns. The concentration effect on the value of M_w can be neglected when considered with second virial coefficient data for linear polystyrene in THF.[17] The concentration effect on $\langle S^2 \rangle$ can also be ignored. In the region $V_e <$ 19.6 cm^3 (the left dashed line), the $M_w - V_e$ relation

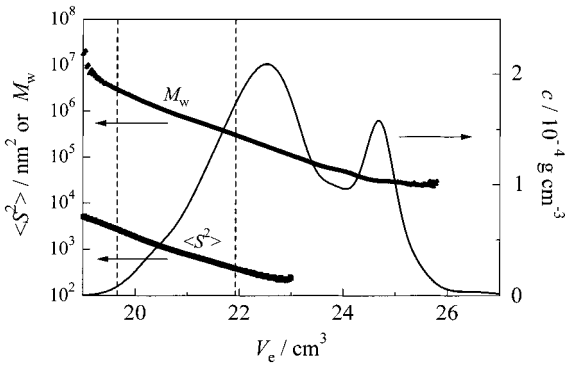

Figure 3. Plots of M_w, $\langle S^2\rangle$, and c vs V_e for comb polystyrene CS25−35.

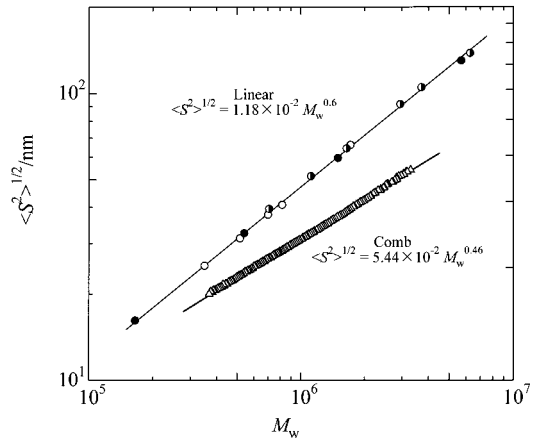

Figure 4. Molecular weight dependence of $\langle S^2\rangle$ for linear polystyrene (○, this work; ●, Schulz and Baumann;[17] ◑, Park et al.[18]) and comb polystyrene CS25−35 in THF.

deviates from the nearly linear relation for $V_e > 19.6$ cm^3 because of the exclusion limit of the GPC columns. The $\langle S^2\rangle^{1/2}$ values for $V_e > 21.9$ cm^3 (the right dashed line) are less than 20 nm, the lowest limit for the determination of $\langle S^2\rangle$ with adequate precision. Thus, we use the data for 19.6 cm^3 ≤ V_e ≤ 21.9 cm^3 in the following analysis.

The triangles in Figure 4 show the $\langle S^2\rangle^{1/2}$ data for comb polystyrene CS25−35 in THF. The figure includes the data for linear polystyrene in Table 2 (unfilled circles) along with those determined by Schulz and Baumann[17] (filled circles) and Park et al.[18] (half-filled circles). They fall on a straight line, which is expressed by

$$\langle S^2\rangle^{1/2} = 1.18 \times 10^{-2}\, M_w^{\,0.6} \quad \text{(nm, linear)} \qquad (1)$$

The exponent 0.6 agrees with the Flory value, which is commonly observed for linear flexible polymers in good solvents. The $\langle S^2\rangle^{1/2}$ values for the comb polymer (triangles) are systematically smaller than those for linear polystyrene as expected for highly branched polymers. They can be fitted approximately by a straight line with slope 0.46, which is much smaller than the Flory exponent for linear chains. The molecular weights from 4×10^5 to 3×10^6 correspond to 6 to 50 in terms of the number of the junction points p in a molecule.

Figure 5 shows the plots of $\langle S^2\rangle^{1/2}$ vs M_w for the polystyrene centipedes in THF. The molecular weight range for any centipedes is narrower than that for the comb polymer, being p from 3 to 6 for GS60−15, from 4 to 12 for GS40−25, and from 6 to 9 for GS15−35. Importantly, $\langle S^2\rangle^{1/2}$ decreases with increasing r (in Table 1) when compared at the same molecular weight. The data for GS40−25 can be fitted by a solid straight line with slope 0.52, which is also smaller than the Flory exponent for linear polystyrene.

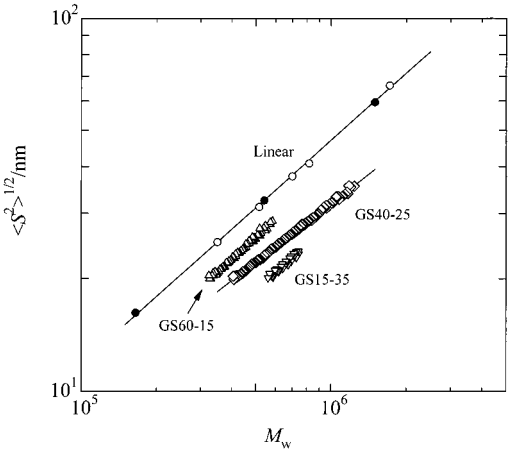

Figure 5. Molecular weight dependence of $\langle S^2\rangle$ for linear polystyrene (symbols are the same as those in Figure 1) and the indicated polystyrene centipedes in THF.

Discussion

The ratio g_S of $\langle S^2\rangle$ for a branching polymer to that for the linear polymer with the same molecular weight is often used to characterize the degree of branching or the segment density in the molecule. Some equations of g_S for several types of comb polymer were derived,[19−23] assuming the Gaussian bond probability. However, none of them is applicable to our centipedes. We therefore calculated g_S for Gaussian comb polymers having p junction points with functionality f, i.e., those in which $(f-2)$ side chains are connected at each junction point ($f = 3$ for the comb and $f = 4$ for the centipedes). The result reads (see Appendix A)

$$g_s = \frac{1}{[(f-2)rp + p + 1]^3}\{(f-2)p[3p(f-2)-2]r^3 + (f-2)p(p+1)[(f-2)(p-1)+3]r^2 + (f-2)p(p+1)(2p+1)r + (p+1)^3\} \qquad (2)$$

In the case of $f = 3$, this equation reduces to the Berry-Orofino equation[21] for normal comb polymers. For $p = 1$ and $r = 1$, it gives the Zimm−Stockmayer equation[19] for star polymers with f arms. On the other hand, when p is much larger than unity, we obtain

$$g_s = \frac{3(f-2)}{p}\left(\frac{r}{r+1}\right)^2 + \frac{1}{r+1} \qquad (3)$$

which is known as Orofino's equation[20] (for $f = 3$).

From eq 2, g_S can be calculated if f, p, and r are given. The values r for our samples are given in Table 1, and p can be calculated from M_w with M_{side} and M_{con} in the table. The dashed line in Figure 6 represents the $\langle S^2\rangle^{1/2}$ values calculated for the comb polystyrene CS25−35 from eq 2 with $\langle S^2\rangle^{1/2}$ for linear polystyrene (eq 1). When the molecular weight is lower than 10^6, i.e., when $p < 18$, the calculated values agree well with the experimental data. This suggests that g_S in the good solvent system is very close to that under Θ conditions when the branching degree is not high. We note that for star polymers with $f < 10$, g_S values in good solvents are known to coincide with those calculated from Gaussian

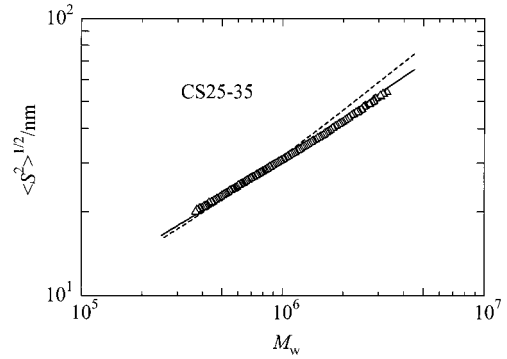

Figure 6. Comparison of experimental $\langle S^2\rangle$ (triangles) for CS25−35 with the values calculated for the flexible discrete comb (dashed line) and the wormlike comb model (solid line).

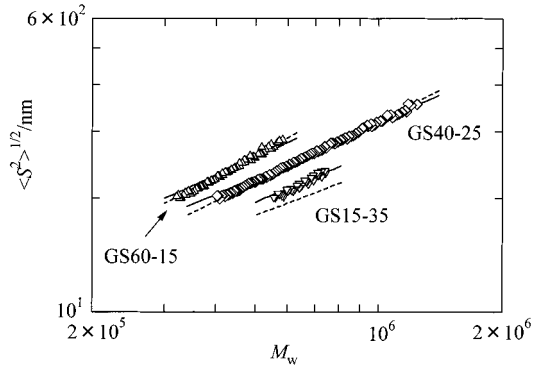

Figure 7. Comparison between experimental values of $\langle S^2\rangle$ (symbols) for the polystyrene centipedes indicated and those calculated for the flexible discrete comb (dashed lines) and the wormlike comb model (solid lines).

models.[24−27] For $M_w > 10^6$, however, the dashed line deviates upward from the data points progressively with increasing molecular weight. Hence, eq 2 fails to explain the molecular dependence of $\langle S^2\rangle$ for CS25−35.

Figure 7 compares the $\langle S^2\rangle^{1/2}$ data for the centipedes with the values (dashed lines) calculated from eq 2 ($f = 4$) with eq 1. The dashed lines for GS60−15 and GS40−25 closely fit the plotted points in the molecular weight range examined, whereas that for GS15−35 deviates downward from the data points. This deviation may be attributed to the stiffness caused by the high side chain density in GS15−35 compared to the other samples.

To estimate the backbone stiffness of our polymers, we calculated $\langle S^2\rangle$ of a wormlike comb (including normal combs and centipedes) whose main chain and side chains have Kuhn segment length λ^{-1} and λ_s^{-1}, respectively. The main chain consists of $(p + 1)$ connectors of contour length L_c linearly linked at p junction points, i.e., the contour length L of the main chain equals $(p + 1)L_c$. At each junction point, $(f - 2)$ side chains of contour length L_s are connected to the main chain by completely flexible joints. Although such flexible joints may not be realistic, the direction of the side chains at junction points does not matter for comb polymers with flexible side chains. A similar model was proposed by Terao et al.[4,5,28] to examine the effect of the thickness on $\langle S^2\rangle$ of polymacromonomers. We note that, although linear polystyrene is better modeled by the helical wormlike chain,[29] its helical nature is weak.

The resulting expression for $\langle S^2\rangle$ consists of two parts, the contributions $\langle S^2\rangle_s$ and $\langle S^2\rangle_m$ from the side chains and the main chain, respectively (see Appendix B)

$$\langle S^2\rangle = \langle S^2\rangle_s + \langle S^2\rangle_m \tag{4}$$

where

$$\langle S^2\rangle_s = \frac{(f-2)p}{L_t^2}\left\{L_s^2\left[\frac{L_s}{6\lambda_s} - \frac{1}{4\lambda_s^2} + \frac{1}{4\lambda_s^3 L_s} - \frac{1}{8\lambda_s^4 L_s^2}(1-e^{-2\lambda_s L_s})\right] + L_s(L_t - L_s)\left[\frac{L_s}{2\lambda_s} - \frac{1}{2\lambda_s^2} + \frac{1}{4\lambda_s^3 L_s}(1-e^{-2\lambda_s L_s})\right]\right\} \tag{5}$$

and

$$\langle S^2\rangle_m = \frac{1}{L_t^2}\left\{\frac{L^3}{6\lambda} - \frac{L^2}{4\lambda^2} + \frac{L}{4\lambda^3} - \frac{1}{8\lambda^4}(1-e^{-2\lambda L}) + (f-2)L_s\left[\frac{2p+1}{p+1}\frac{pL^2}{6\lambda} - \frac{pL}{2\lambda^2} + \frac{p}{2\lambda^3} - \frac{1}{2\lambda^3}\frac{e^{-2\lambda L_c}}{1-e^{-2\lambda L_c}}(1 - e^{2\lambda L_c p})\right] + (f\text{-}2)^2 L_s^2\left[p(p-1)\left(\frac{L}{6\lambda} - \frac{1}{4\lambda^2}\right) + \frac{1}{2\lambda^2}\frac{e^{-2\lambda L_c}}{1-e^{-2\lambda L_c}}\left(\frac{p - e^{-2\lambda L_c p}}{1-e^{-2\lambda L_c}}\right)\right]\right\} \tag{6}$$

with L_t being the total contour length given by $L_t = (f - 2)pL_s + (p + 1)L_c$. In the case of, $p \gg 1$ and $\lambda L_c \ll 1$, eq 4 for $f = 3$ reduces to the equation of Terao et al.[28]

In a comblike molecule, the main chain may be stiffened by the interaction between side chains, but analyses of intrinsic viscosity $[\eta]$ and translational diffusion coefficient data for polymacromonomers suggest that each polystyrene side chain has an end-to-end distance comparable to that of the free linear chain with the same contour length.[6,30] In other words, the stiffness of the side chain may not differ much from that of the linear chain whose dimensions are characterized by a Kuhn length of 2 nm and a linear mass density M_L of 390 nm^{-1}.[31] Thus, with $\lambda_s^{-1} = 2$ nm, $M_L = 390$ nm^{-1} (for both main chain and side chains), and the known p values, we searched for λ^{-1} that gives the closest agreement between the $\langle S^2\rangle$ for the polystyrene comb CS25−35 and those calculated from eq 4 with eqs 5 and 6. The solid line in Figure 6 represents the values calculated with $\lambda^{-1} = 5.5$ nm, a value more than twice as large as λ_s^{-1}. Its close fit to the data points shows that the wormlike model is preferable to the discrete flexible-chain model for the comb polymer and that the main chain is stiffened by the congestion of the side chains.

Similar comparisons are shown for the centipedes in Figure 7, where we have used $M_L = 390$ nm^{-1} and $\lambda_s^{-1} = 2$ nm again and chosen λ^{-1} values of 4.5 nm for GS60−15, $\lambda^{-1} = 5.5$ nm for GS40−25, and $\lambda^{-1} = 8.5$ nm for GS15−35 to best fit the data points for the respective polymers. The close fits of the solid lines to the data points substantiate that the main chains of the centipedes have higher stiffness for larger r (see Table 1). Since r represents the crowdedness of the side chains, this demonstrates that the side chain density is essential to stiffening the main chains of the comblike polymer.

Conclusion

The method of Iatrou et al.[15] was applied to synthesize a comb polymer sample with uniform side chains

equally spaced along the main chain but with broad (most probable) distribution in the length of the main chain. The molecular weight dependence of $\langle S^2\rangle$ of the comb polystyrene in THF was obtained using a GPC system equipped with MALLS and RI detectors. The $\langle S^2\rangle$ values for the comb polymer for $p < 18$ were represented by the calculated values with g_S for the Gaussian comb and $\langle S^2\rangle - M_w$ relation for linear polystyrene in THF. The calculated values for the centipedes also fit the experimental data for $r < 1$. However, $\langle S^2\rangle$ of the comb for $p > 18$ and that of the centipedes for $r > 1$ could not be represented by the calculated values. The wormlike comb polymer model whose main and side chains have different Kuhn lengths explained all the $\langle S^2\rangle$ data obtained. From the comparison between the experimental and calculated values, it was found that the stiffness of the main chain of the centipedes increases with r. However, the intramolecular excluded volume effects were ignored in the above analyses. To examine these effects, measurements on the Θ solvent system are in progress.

Acknowledgment. We thank Professor Takashi Norisuye in Osaka University for valuable comments on this manuscript. Y.N. thanks Dr. Ken Terao at Ritsumei University for fruitful discussions on the wormlike comb model. This work was supported by the U.S. Army Research Office (DAAG55-98-1-0005). We also acknowledge support by the National Science Foundation for an instrument grant (DMR-9802853) that allowed the purchase of the GPC-MALLS system.

Appendix A. Derivation of Equation 2.

The general expression of g_S for flexible branched polymers is given as[32,33]

$$g_S = \frac{1}{N_t^3}\left[\sum_i (3N_t n_i^2 - 2n_i^3) + 6\sum_{i<j}\sum n_i n_{ij} n_j\right] \quad \text{(A1)}$$

Here, N_t is the total segment number in the molecule, n_i and n_j are the numbers of segments in the ith and jth subchains, respectively, and n_{ij} is the number of segments in the subchains lying between the ith and jth subchains. The summations are taken over all the subchains.

The first term in the brackets of eq A1 for regular comblike polymers made of side chains and connectors with fixed numbers of segments n_s and n_c, respectively, gives

$$p(f-2)(3N_t n_s^2 - 2n_s^3) + (p+1)(3N_t n_c^2 - 2n_c^3) \quad \text{(A2)}$$

where p and f represent the number and the functionality of the junction points in the molecule.

Considering the three cases: 1. Both ith and jth subchains are the side chains. 2. both ith and jth subchains are the connectors. 3. One of the ith and jth subchains is the side chain and the other is the connector; the second term in the brackets in eq A1 gives

$$p(p^2-1)n_c[(f-2)n_s + n_c]^2 \quad \text{(A3)}$$

Substituting eqs A2 and A3 into eq A1 and considering $N_t = p(f-2)n_s + (p+1)n_c$ and $r = n_s/n_c$, we obtain eq 2.

Appendix B. Derivation of Equations 4 and 5.

The mean-square radius of gyration for branched polymers made of wormlike subchains is given by[34,35]

$$\langle S^2\rangle = \frac{1}{2L_t^2}\sum_p\sum_q \int_0^{L_p} dr_p \int_0^{L_q} dr_q \langle R^2(r_p,r_q)\rangle \quad \text{(B1)}$$

Here, L_t denotes the total contour length given by $\sum_p L_p$ and $\langle R^2(r_p, r_q)\rangle$ the mean-square distance between two points at r_p and r_q on the pth and qth subchains, respectively. The variables r_p and r_q represent the contour distance from one end and take values from 0 to the lengths of the subchains, L_p and L_q, respectively.

When the side chains are connected by free-rotating joints to the main chain, eq B1 for the wormlike comb is represented by the following equation:

$$\langle S^2\rangle = \frac{1}{L_t^2}(I_1 + I_2 + I_3 + I_4) \quad \text{(B2)}$$

Here, I_1, I_2, I_3, and I_4 represent the contributions, respectively, from the following cases: 1. r and r' are on the main chain

$$I_1 = \int_0^L dr \int_r^L dr' \langle R^2(r,r')\rangle_m \quad \text{(B3)}$$

2. r_i and r_i' are on the ith side chain

$$I_2 = \sum_{i=1}^{N} \int_0^{L_s} dr_i \int_{r_i}^{L_s} dr_i' \langle R^2(r_i,r_i')\rangle_s \quad \text{(B4)}$$

3. r is on the main chain and r_i is on the ith side chain

$$I_3 = \sum_{i=1}^{N} \int_0^L dr \int_0^{L_s} dr_i [\langle R^2(r,r_{i0})\rangle_m + \langle R^2(r_{i0},r_i)\rangle_s] \quad \text{(B5)}$$

4. r_i and r_j are on the ith and jth side chains, respectively.

$$I_4 = \sum_{i=1}^{N-1}\sum_{j=i+1}^{N} \int_0^{L_s} dr_i \int_0^{L_s} dr_j [\langle R^2(r_i,r_{i0})\rangle_s + \langle R^2(r_{i0},r_{j0})\rangle_m + \langle R^2(r_{j0},r_j)\rangle_s] \quad \text{(B6)}$$

Here, N is the number of the side chains, L and L_s are the length of the main and the side chains, respectively, and r_{i0} and r_{j0} represent the positions of the junction points at which ith and jth side chains, respectively, connect with the main chain. The subscripts m and s represent the contributions from the main and the side chains, respectively. These terms can be calculated using $\langle R^2(r, r')\rangle$, the mean-square distance between two contour points r and r' on a wormlike chain[33,36] with Kuhn's segment length λ^{-1}:

$$\langle R^2(r,r')\rangle = \frac{|r-r'|}{\lambda} - \frac{1}{2\lambda^2}[1 - \exp(-2\lambda|r-r'|)] \quad \text{(B7)}$$

Substituting eq B2 with eqs B3−B6 after carrying out the integrations and summations, we obtain eq 4 with eqs 5 and 6.

References and Notes

(1) Wintermantel, M.; Schmidt, M.; Tsukahara, Y.; Kajiwara, K.; Kohjiya, S. *Macromol. Rapid Commun.* **1994**, *15*, 279.
(2) Wintermantel, M.; Gerle, M.; Fischer, K.; Schmidt, M.; Wataoka, I.; Urakawa, H.; Kajiwara, K.; Tsukahara, Y. *Macromolecules* **1996**, *29*, 978.
(3) Nemoto, N.; Nagai, M.; Koike, A.; Okada, S. *Macromolecules* **1995**, *28*, 3854.

(4) Terao, K.; Takeo, Y.; Tazaki, M.; Nakamura, Y.; Norisuye, T. *Polym. J.* **1999**, *31*, 193.
(5) Terao, K.; Nakamura, Y.; Norisuye, T. *Macromolecules* **1999**, *32*, 711.
(6) Terao, K.; Hokajo, T.; Nakamura, Y.; Norisuye, T. *Macromolecules* **1999**, *32*, 3690.
(7) Kawaguchi, S.; Akaike, K.; Zhang, Z.-M.; Matsumoto, H.; Ito, K. *Polym. J.* **1998**, *30*, 1004.
(8) Shiokawa, K.; Itoh, K.; Nemoto, N. *J. Chem. Phys.* **1999**, *111*, 8165.
(9) Decker, P. D. *Makromol. Chem.* **1969**, *125*, 136.
(10) Noda, I.; Horikawa, T.; Kato, T.; Fujimoto, T.; Nagasawa, M. *Macromolecules* **1970**, *3*, 795.
(11) Berry, G. C. *J. Polym. Sci.: A-2* **1971**, *9*, 687.
(12) Candau, F.; Rempp, P. *Eur. Polym. J.* **1972**, *8*, 757.
(13) Strazielle, C.; Herz, J. *Eur. Polym. J.* **1977**, *13*, 223.
(14) Watanabe, H.; Amemiya, T.; Shimura, T.; Kotaka, T. *Macromolecules* **1994**, *27*, 2336.
(15) Iatrou, H.; Mays, J. W.; Hadjichristidis, N. *Macromolecules* **1998**, *31*, 6697.
(16) Huglin, M. B. In *Polymer Handbook*, 3rd ed.; Brandrup, J.; Immergut, E. H. Eds.; Wiley-Interscience: New York, 1989.
(17) Schulz, G. B.; Baumann, H. *Makromol. Chem.* **1968**, *114*, 122.
(18) Park, S.; Chang, T.; Park, I. H. *Macromolecules* **1991**, *24*, 5729.
(19) Zimm, B. H.; Stockmayer, W. *J. Chem. Phys.* **1949**, *17*, 1301.
(20) Orofino, T. A. *Polymer* **1961**, *2*, 305.
(21) Berry, G. C.; Orofino, T. A. *J. Chem. Phys.* **1964**, *40*, 1614.
(22) Kurata, M.; Fukatsu, M. *J. Chem. Phys.* **1964**, *41*, 2934.
(23) Casassa, E. F.; Berry, G. C. *J. Polym. Sci.: A-2* **1977**, *4*, 881.
(24) Douglas, J. F.; Roovers, J.; Freed, K. F. *Macromolecules* **1990**, *23*, 4168.
(25) Grest, G. S.; Fetters, L. J.; Huang, J.; Richter, D. *Adv. Chem. Phys.* **1996**, *94*, 67.
(26) Okumoto, M.; Nakamura, Y.; Norisuye, T.; Teramoto, A. *Macromolecules* **1998**, *31*, 1615.
(27) Okumoto, M.; Tasaka, Y.; Nakamura, Y.; Norisuye, T. *Macromolecules* **1999**, *32*, 7430.
(28) Terao, K.; Nakamura, Y.; Norisuye, T. In *Molecular Interactions and Time-Space Organization in Macromolecular Systems*; Morishima, Y., Norisuye, T., Tashiro, K., Eds.; Springer: Berlin, 1999.
(29) Yamakawa, H. *Helical Wormlike Chains in Polymer Solutions*; Springer: Berlin, 1997.
(30) Terao, K.; Hayashi, S.; Nakamura, Y.; Norisuye, T. *Polym. Bull.* **2000**, *44*, 309.
(31) Norisuye, T.; Fujita, H. *Polym. J.* **1982**, *14*, 143.
(32) Kataoka, S. *Busseiron Kenkyu* **1953**, *66*, 402.
(33) Yamakawa, H. *Modern Theory of Polymer Solutions*; Harper and Row: New York, 1971.
(34) Mansfield, M. L.; Stockmayer, W. H. *Macromolecules* **1980**, *13*, 1713.
(35) Fujii, M.; Nagasaka, K.; Yamakawa, H. *J. Chem. Phys.* **1982**, *77*, 986.
(36) Porod, G. *J. Polym. Sci.* **1953**, *10*, 157.

MA0007076